Simulated Images of Intraocular Lens Negative Dysphotopsia and Visual Phenomena

MICHAEL J. SIMPSON

Simpson Optics LLC, Arlington, Texas 76012, USA
Corresponding author: mjs1@outlook.com

This is the Accepted Manuscript for the Journal of the Optical Society of America A, Vol. 36, No. 4, B44 - B51, April 2019. The final published version has small changes.
https://doi.org/10.1364/JOSAA.36.000B44

Received XX Month XXXX; revised XX Month, XXXX; accepted XX Month XXXX; posted XX Month XXXX (Doc. ID XXXXX); published XX Month XXXX

Simulated images were generated using an extended source to illustrate peripheral dark shadows in pseudophakic eye models. The shadows are a consequence of the intraocular lens being much smaller than the natural crystalline lens, which limits the extent of the focused image. Compensation is made for the cosine intensity falloff due to pupil obliquity, and the images are envisaged as being displayed on polar plots of visual angle, corresponding to approximate retinal locations. Additional retinal illumination from light missing the lens reduces the shadow effect as the pupil diameter increases, in agreement with clinical observations. Lenses with two different cross-sectional profiles were evaluated, which both have shadows at about 85^0, but with different characteristics. The iris thickness was found to affect the shadows by occluding peripheral rays. Images were also generated for a point source with a 5 mm pupil, where a double image is created for visual angles as low as 50^0, which may contribute to visual phenomena at night. This type of modelling may help with patient evaluations and discussions.

http://dx.doi.org/10.1364/AO.99.099999

1. INTRODUCTION

Cataract surgery is one of the most common surgical procedures, and it is highly successful. Some patients may see unwanted visual phenomena following the surgery, and although these are generally easily tolerated, the visual locations, and the magnitude of the effects, are rarely measured objectively. Detailed tests are sometimes used with *multifocal* IOLs, to characterize their distinctive visual phenomena due to the presence of multiple lens powers [1], but these are usually evaluations at small visual angles, and they are typically not used for monofocal IOLs.

An exploration into the cause of "negative dysphotopsia", where patients report seeing a bothersome dark shadow in their peripheral visual field, led to the observation that there appears to have been little research into "far peripheral vision" in general , which is probably a contributing factor to the lack of measurement methods. The main objective clinical test at large visual angles is "perimetry". This is widely used to characterize pathologies of the visual and neurological systems, although often for only modest visual angles. It is not typically used to measure routine visual performance, and it is not intended to evaluate unwanted visual phenomena. There are no standard clinical test methods to record the visual angles and other properties of unwanted visual phenomena while they are being observed, at even modest visual angles. With "dark shadows", or "negative dysphotopsia", a military salute, where the hand is held up against the temporal side of the head near the eyebrow, seems to be a useful test when evaluating it [3, figure 3]. The hand identifies the visual region of interest, and it also typically blocks the source of light that causes the shadow.

The primary cause of negative dysphotopsia is probably due to the intraocular lens (IOL) in the pseudophakic eye being very much smaller than the natural crystalline that it replaces. This simple explanation was not even considered when causes of the phenomenon were initially discussed [4,5]. At the time, it was not clear that very little was known about far peripheral vision [2], and IOLs had been used already for many years, with the IOL diameter remaining fairly constant (usually about 6mm, but with a range from 5 to 7mm). Various other things had changed though since the start of the widespread use of IOLs, particularly the quality of the surgery, and the use of foldable lenses, and these left the ocular tissue surrounding the lens much clearer than before. When the relative dimensions of the natural lens and the IOL are compared (Figure 1 [6]), it is surprising that there are not more observations of visual changes.

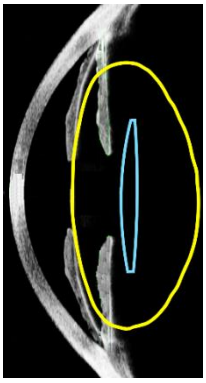

Fig. 1 Superposition of preoperative and postoperative OCT images for the same eye (age 67, corneal power 43.5D, axial length 21.5mm). The overall shape of the crystalline lens is sketched using a published example [7, Fig 9], since only the anterior surface is visible.

Unwanted visual phenomena at large angles are rarely bothersome, which seems to have led to the entire visual region being neglected as a research topic, even for the phakic eye [2]. IOLs themselves developed pragmatically as a replacement for the natural crystalline lens, with the greatest emphasis being placed on providing focused foveal vision. Surgical methods and IOL characteristics improved over time, and although the surgery is widely performed, there are occasionally cases where a patient has an excellent surgical result, but they are bothered by peripheral dark shadows with small pupils (negative dysphotopsia), or by night-time visual phenomena with larger pupils at night (positive dysphotopsia). Both these situations are evaluated here.

An earlier paper in this journal evaluated how a peripheral double image may be perceived as a shadow [8], and a later paper used the word "vignetting", which clarified that the cause of the "shadow" is primarily because the IOL is so small that at large angles the light no longer passes through the IOL, and the main image goes dark [9]. However, those methods only evaluated ray locations, not ray intensities, to illustrate general properties of the shadow. This approach was also used in a more recent paper in the clinical literature [10]. However, the inherent dimming at large visual angles of the primary image created by the IOL, still does not appear to be widely recognized by clinicians. A dark shadow might still be described to a patient as being of "uncertain etiology", and being "multifactorial in nature" [5,11,12]. Alternative methods for presenting the raytrace evaluations are considered here, with the expanded use of simulated images.

The clinical reports relating to dark shadows do not identify the characteristics of the visual scene in the periphery as being important, and the most prominent characteristic is simply a bothersome "shadow". However, even basic parameters of the shadow, such as the visual angle at which it appears, are not known. It is possible that if additional clinical details were available then that may clarify what causes the phenomenon to be so bothersome to certain patients. Vision generally responds to changes, rather than to constant intensity. Despite this concern, a shadow created by a constant intensity object is found here to be a powerful method for summarizing the overall visual effect in the far periphery. It captures the primary characteristics of the phenomenon, which is a variation of intensity, unlike the more common measures of vision which evaluate image detail. The image is not isoplanatic, and the point spread function (PSF) varies continuously across the imaging region, particularly in the radial direction.

The use of a *ganzfeld* object, where light enters the eye from every angle possible, was described in an earlier paper [4], but an error was made in some calculations there. This was rectified in a later paper [10], but the original uncorrected reference is still a primary source of information about negative dysphotopsia. The main error was to not include rays from every angle, which is probably a consequence of how difficult it is to set up this type of evaluation in standard raytrace software. All the rays that pass through the pupil need to be included, and Zemax, which was used in that study, does not have a convenient way to arrange this for nonsequential raytracing. Also, near the edge of an IOL, rays from the same input beam can both pass through the IOL, and miss the IOL. This is related to the vignetting characteristic at the edge of the IOL. However, something that is perhaps unexpected is that it is not rays from a single input beam that create the overall image characteristics. Rays that miss the IOL start having an effect at low input angles, and there is one set of rays that create the focused image, and a different set of rays that create a more peripheral "image" from light that misses the lens. This has a lower magnification because the light does not pass through the IOL. Negative dysphotopsia is also primarily associated with small pupils, and it is shown here that as the pupil opens up, the shadow effect diminishes, which is consistent with clinical reports.

A related effect is present for large pupils, where a point source at night can create a double image. This can occur even for relatively modest visual angles, and images are created that illustrate this. Visual phenomena are often reported at night by users of IOLs, and this may be a contributing factor, though it is not usually mentioned in discussions of possible causes.

2. MATERIALS AND METHODS

Previous evaluations [9,10,13,14] of negative dysphotopsia have involved raytracing calculations, but these have rarely included simulated images of what a patient might see in the periphery. One limitation of drawings that show rays is that they typically do not also indicate the relative intensity of the ray (Fig. 2). Light that passes from one medium to another experiences the effect of a Fresnel reflection, where part of the energy is reflected rather than transmitted, and this effect increases with increasing incident angle, and increasing refractive index. The effect that the ray density has on image intensity, where imaging aberrations defocus the light at the retina, is also difficult to visualize from a ray drawing.

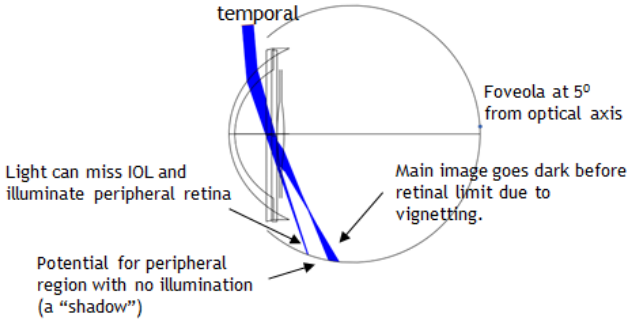

Fig. 2 Raytrace plot. Right eye from above. 2.5mm pupil. Input 90^0 to visual axis (85^0 to optical axis). (The main parameters, with units in mm, are: Cornea r1=7.76, cc1=-0.26, t=0.55, r2 =6.36, cc2=-0.24. Cornea to pupil =3.45. Pupil to IOL = 0.5. IOL r1 = 19.69, t=0.66, r2=-19.69. Axial length= 23.5. Cornea index=1.376. Ocular fluid index=1.336. IOL index=1.55. r=radius, cc=conic constant, and t=axial distance).

However, displaying raytracing results as an image has particular complications for the far peripheral vision region of the eye, particularly because the image is formed on the highly curved surface of the retina. An earlier evaluation created simulated images for a distant square window, and developed a method to flatten the image out for comparative evaluations [8]. More recently, retinal locations were converted instead to input visual angles for the analysis of individual rays [10], and that is the method that is used here, but expanded now to display an image that is represented in terms of input visual angle.

An average eye with a simple high refractive index acrylic IOL was used for calculations. The main details of this eye have been described previously [10], and the eye is depicted in Fig. 1 with light rays entering the eye at 85 degrees to the optical axis. The foveola in an average eye is displaced 5^0 temporally, and this value is added to the input angles to give the angle to the visual axis (which is 90 degrees in Fig 1). No adjustment is made for the vertical location of the foveola. The pupil is decentered nasally by 0.17 mm, which is an average amount, and diameters from 2.5 – 5 mm are considered. Rays are traced up to an angle that is 95^0 to the optical axis. The Zemax raytrace software was used for the calculations (Radiant Zemax, Redmond, WA).

One characteristic of the eye that was not included in earlier calculations is the thickness of the iris, which is normally just modeled as a thin structure in lens design and analysis software. The rays enter the eye very obliquely here, and the possibility that the anterior iris surface might obstruct the light [2] was evaluated. This was modeled as an aperture with an opaque surround, 0.5 mm in front of the pupil plane, and with a diameter 2mm larger than the pupil, using values recently published [6]. This was found to have an effect for smaller pupils, and the main images were generated using this model.

To permit input rays to exceed 90^0 in Zemax, and image rays to exceed 90^0 on a hyperhemispheric retinal surface, the model eye was set up so that it could be rotated about a vertical axis. A macro was used to record the coordinates of ray intersections with the retina for a large number of object points at 6 meters from the eye. The macro takes advantage of the "ray aiming" capability of the "sequential" Zemax raytrace method to find the location of the iris boundary for rays from each object point, and then launches a set of rays that are equally spaced in angle. A separate "polarization" routine was then also used to calculate the fraction of each focused light ray that reached the retina, after Fresnel reflections were removed, and this was also saved. The retinal ray intersections were then read into Matlab for processing (Mathworks, mathworks.com).

The relationship between input angles and corresponding retinal locations was generated by tracing a set of chief rays that pass through the center of the pupil. The angles subtended at the second nodal point were calculated, using the nodal point value calculated by Zemax, and this is plotted in Fig. 3(a). This is a very linear relationship to about 70 degrees, before there is a modest change. Aberrations alter the effective image location at large angles, and eventually the chief ray does not pass through the IOL. The extrapolated linear curve is used here for all the retinal locations to give the relative relationship between different regions of the peripheral image.

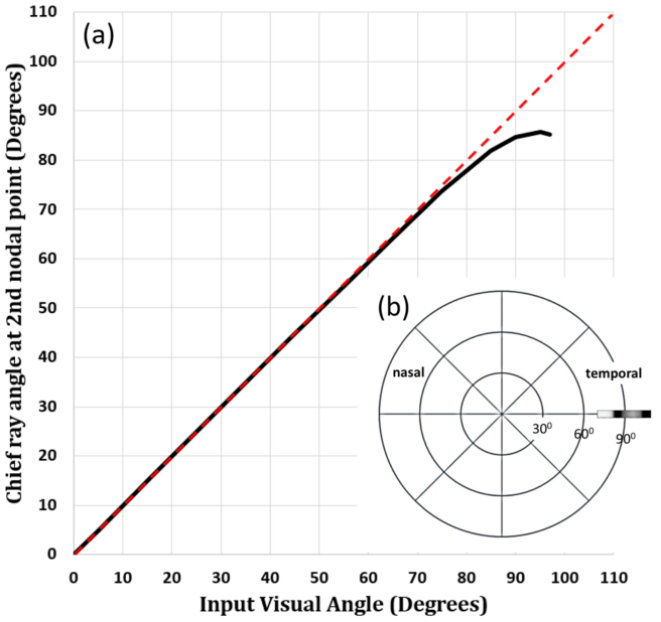

Fig. 3 (a) Chief ray input angle vs retina intersection point measured as the angle subtended at the 2nd nodal point. (b) Polar plot with image.

Fig 4 illustrates how the retinal image locations are converted back out of the eye to approximate relative optical input angles on a polar plot (Fig. 3(b)), using simply the angular location of each retinal location relative to the 2nd nodal point of the pseudophakic eye. This method addresses the fact that there is not a 1:1 relationship between object and image points for the pseudophakic eye, and that what is important is where the light *appears* to come from in object space, rather than where it actually does come from. This is different to the phakic eye, where aberrations are lower and the image does not bifurcate because the edge of the lens is never exceeded.

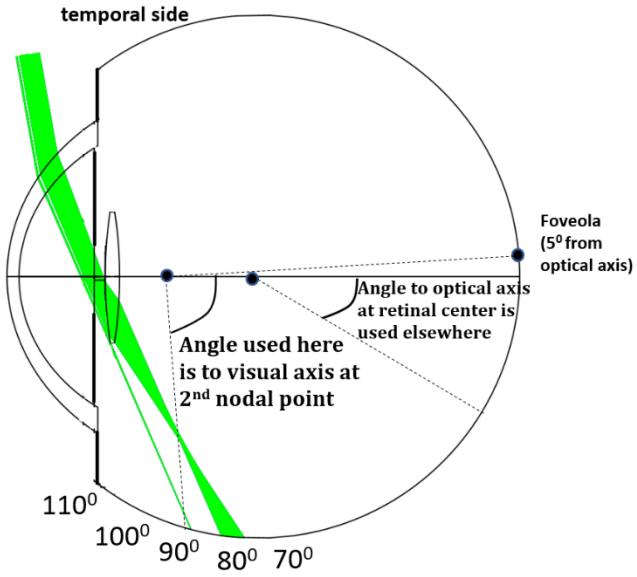

Fig. 4. (a) Retinal locations are scaled using a linear extrapolation of the relationship for the chief ray. This permits light that originates from different directions to be evaluated as a single representative image.

Earlier publications have used the center of the retinal sphere as the reference point for angular measurements at the retina [15], and this is also illustrated in Fig 4. That also creates a very linear relationship to the input angle for lower angles, which can also be expressed as the distance along the retina, but the numerical values for either of those methods are difficult to interpret. The use of the second nodal point gives angular values that can be more directly related to the input angles.

Polar plots are already used in ophthalmology to represent input visual angles, and the use here attempts to simulate the visual effect at the image, while also representing it in object space (Fig. 3(b)). The polar plot is also extended to the limit of vision, at about 110 degrees. The outer circumferential circle is not drawn in Fig 3(b) to emphasize how different this is to standard clinical practice. A typical ophthalmic plot only extends to 90 degrees, with measurements only rarely made to large visual angles. This evaluation is something that can be done using a theoretical model for the eye, but it is not possible using standard clinical test methods. The simulated image is actually created as a rectangle, with horizontal and vertical angular dimensions, rather than as a true polar image, since its main purpose here is as a visual representation of the shadow.

The Zemax raytrace software does not have the ability to directly generate the types of images that are of interest here, and new methods were created using the sequential raytrace capabilities of Zemax. Special optical surfaces were created for the IOL using the "user defined surface" capability, so that rays that passed through the IOL, and rays that missed the IOL, could both be recorded for the same optical system. Rays striking the lens edge or the haptics were ignored, but these are generally both textured and curved for the IOLs of interest, and the rays are generally scattered and defocused, and directed away from the region of interest.

Published calculations often use a simple lens, where the optical surfaces extended to the edge of the IOL [10]. Evaluations of potential methods to mitigate the effect of negative dysphotopsia using a secondary piggyback IOL in the ciliary sulcus [16], and alternative designs [17], led to the modelling of IOLs with different peripheral features. Two examples are illustrated in Fig 5, where for the higher 1.55 refractive index lens the optical surfaces go to the edge of the physical 6 mm diameter lens. With a lower refractive index lens, some IOL designs have a limited optical surface diameter, and the example in Fig 5(b) with a 1.47 refractive index has both a peripheral cone on the anterior surface, and a posterior peripheral planar region [18]. Physical details like these for IOLs with lower refractive index values are rarely published, but the surfaces have to be steeper with a lower refractive index, which leads to greater physical bulk, which may prevent the lens from being inserted through the smallest of incisions. Reducing the diameter of the lens-like surface, on one or both sides of the lens, can reduce the incision size. The profile in Fig 5(b) is just one example.

Fig. 5 Cross-sectional IOL profiles, with 6mm diameter, for (a) refractive index 1.55, and (b) refractive index 1.47 [18].

To generate the images in Matlab, the rays weighted by their transmitted intensity were added into an array that represented the relative polar locations in object space of the retinal locations. Figure 3(b) illustrates the approximate region of the image on a polar plot. The image is formed within a rectangle, but each point represents a radial angular distance from the optical axis, and an azimuthal rotation from the horizontal. This covers an image region from approximately 70^0-110^0 radially, by approximately $\pm 3^0$ vertically, but calculations were originally made for a much larger vertical angle range in order to capture the effect of the full PSF ($\pm 10^0$). Simulated images were created for a uniformly illuminated hemisphere at 6 meters, for several pupil diameters, and separately for a bright object point at different angles for a 5 mm pupil (to simulate a bright light at night).

Additional weighting of the rays was also used to compensate for the falloff in energy with increasing angle. This effect can be envisaged when considering how the iris appears to become increasingly elliptical with increasing visual angle, with the horizontal opening getting smaller and smaller until eventually there is total occlusion. The transmitting area falls off as an approximate cosine function [19] (Fig. 6), and to counteract this each ray was weighted by 1/(cos (0.8*retinal angle)). This increases the relative intensity of the most peripheral rays for evaluation. A value of approximately 0.9*retinal angle had been found for the effect of pupil obliquity alone for the phakic eye, without considering any additional effects due to aberrations [19].

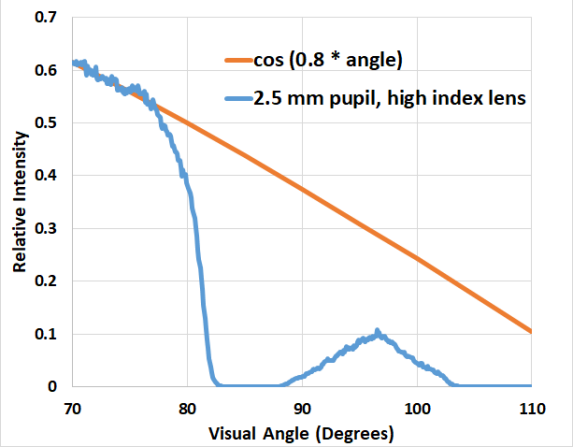

Fig. 6 The relative intensity on the retina declines following an approximate cosine function due to the increasingly elliptical effective profile of the pupil. Original retinal illumination in blue, with normalization curve in orange.

In practice, the mechanism by which the eye compensates for the image getting dimmer in the periphery does not appear to be known [2], and this method compensates only for the optical effect of pupil obliquity. It is possible that any compensation that is also made by the visual system with respect to peripheral darkening may lead to dark shadows being more bothersome to some patients than to others. This scaling addresses the main optical characteristics of the situation, and it provides a standardized image, so that the relative image properties can be evaluated. Each visual image was also scaled independently to approximately fill the available intensity range, and a gamma value of 0.3 was used for display. Plots across the horizontal line of the

intensity image were also created (without the gamma adjustment).

The main images were calculated with the iris decentered nasally by 0.17 mm compared to the optical axis, which is thought to be a typical amount. However, the shadow strength and location was found to vary with iris centration, IOL centration, and IOL tilt, and additional calculations were done that varied these parameters for the high index lens. Images of the PSF were also generated and displayed for the high index lens.

3. RESULTS

Fig 7(a) shows simulated images of the main negative dysphotopsia effects for a high index IOL with an extensive bright object at 6 meters, for several pupil diameters. The intensity across the horizontal axis is plotted at the right side for each image. The IOL cross-section for the high index IOL is depicted in Fig 5(a). The distinct shadow for the smallest pupil arises because the main image goes dark at a location on the retina that corresponds to a visual angle of about 85^0 because the IOL diameter is not large enough to pass any more light. Light also misses the IOL, and it starts missing the lens at a smaller visual angle than the light that creates the last portion of the focused image, but there is a gap between the two illuminated regions. As the pupil diameter increases, however, the light that misses the IOL illuminates the retina at lower and lower "apparent" visual angles, and the visual effect of the dark shadow reduces with increasing pupil diameter. This behavior is consistent with clinical reports of dark shadows [6].

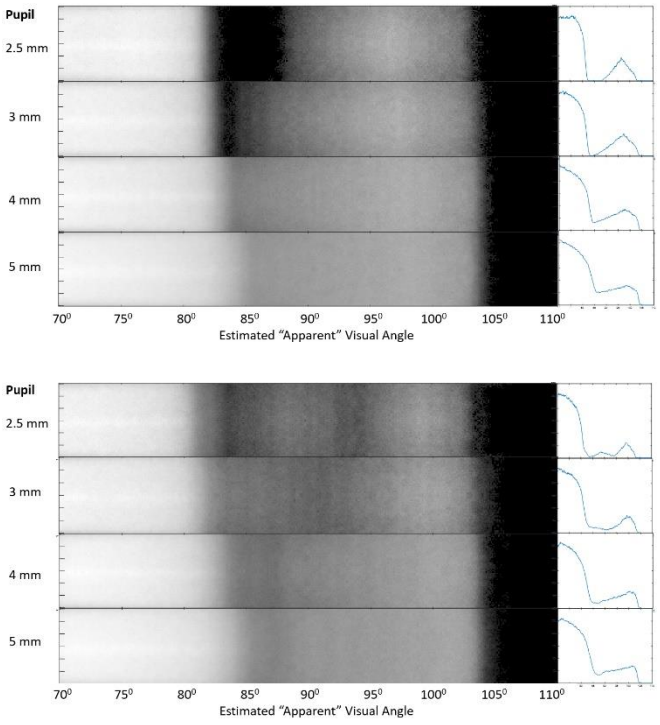

Fig. 7 Image intensity for peripheral retinal region from 70^0-110^0 horizontally and $\pm 3^0$ vertically for different pupil diameters, accompanied by intensity plot along horizontal direction at right. (a) High index IOL. (b) Lower index IOL.

Fig 7(b) shows equivalent simulated images for an IOL that has a lower refractive index (1.47), with the cross-sectional profile illustrated in Fig 5(b). The effective diameter of the optical surface is reduced for this lens.

The images in Fig. 7 were all calculated using a thick iris, and this was found to occlude some rays at very large angles for smaller pupil diameters. This effect is illustrated in Fig. 8, where the two images for the 2.5mm pupil from Fig. 7 are reproduced, along with alternative calculations where a thin iris is used. The use of a thick iris alters the characteristics of both the focused image, and the light that misses the IOL, for both lens types.

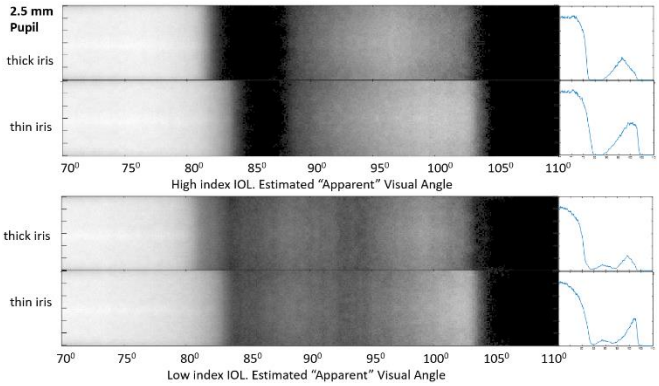

Fig. 8. Images for the 2.5 mm pupil comparing a thick iris to a thin iris, for a high index IOL (top), and low index IOL (bottom).

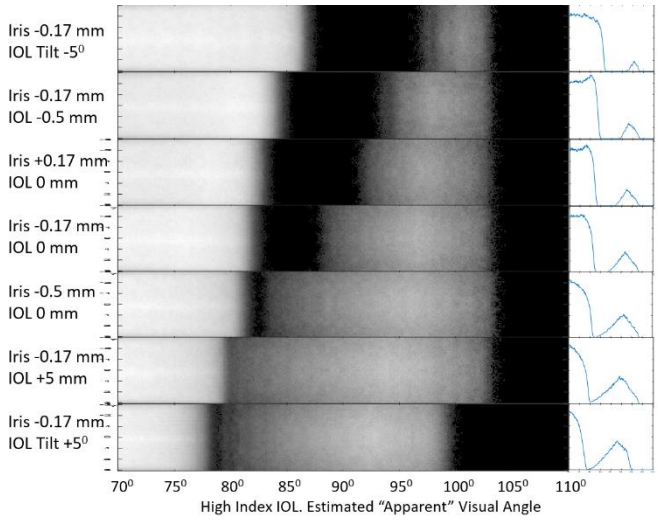

Fig. 9. Images with a 2.5 mm pupil with different iris and lens decentration values, and with IOL tilt about a vertical axis with the IOL centered. The images are displayed in an order that moves the shadow to lower angles. The limited extent of the bottom image is an artifact of the calculation.

The changes in the shadow due to decentration of the iris or IOL, and tilt of the IOL, are illustrated in Fig. 9. The average eye has an iris that is decentered by -0.17 mm compared to the optical axis, which is in the nasal direction, and this is represented by the central image in Fig. 9. Increasing the iris decentration to -0.5 mm reduces the effect of the shadow because more light misses the IOL, and decentering the iris in the opposite direction to +0.17 mm increases

the shadow. With the iris at the standard -0.17 mm decentration, and decentering the IOL by ± 0.5 mm increases these effects, and tilting the IOL by ± 5^0, without decentration, increases the effects even further.

The visual effect of light sources at night is illustrated by PSF images, and these are given in Figure 10 for the high index acrylic lens with a 5 mm diameter pupil. For each pupil diameter, the intensity range of the sub-image is adjusted to fill the full intensity range, and the gamma value is set to 0.3 as before.

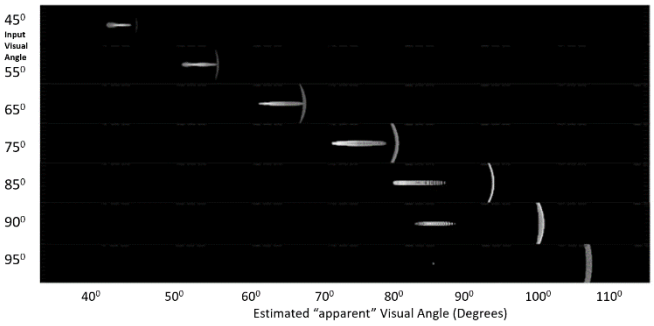

Fig. 10. Images of a point source at different input visual angles for the high index IOL with a 5mm pupil diameter.

4. DISCUSSION

Despite ongoing concerns about negative dysphotopsia, clinical papers tend to state that the etiology is not known [5,12]. The calculations here show, however, that visual effects like these are actually inherent characteristics of the use of IOLs, because the lenses are so much smaller than the natural crystalline lens. Visual acuity in the periphery is very low, however, and scattering from ocular tissue can reduce the effects. Scattering was particularly prevalent in the early days of IOLs, which is probably why negative dysphotopsia was not reported initially.

The characteristics of the simulated shadows are in agreement with general clinical observations by patients, though the actual angles at which the phenomenon is seen are rarely reported. Separately, modelling of the use of a piggyback lens to show how it can reduce the effect of a shadow also agreed with clinical results (but again without angle values) [16]. The modelling here uses both a simple lens edge for a higher index acrylic IOL, and a peripheral flange region for a lower index lens, and these have slightly different intensity profiles. However, the thing that is common to all pseudophakic eyes is that at very large angles the light is no longer focused by the IOL, and shadow phenomena are a possibility. The modeling also shows that when the pupil diameter is increased, the shadow is reduced, which agrees with clinical observations. This happens because light increasingly bypasses the IOL as the pupil diameter increases, which illuminates the main region of the shadow, and this change is sensitive to very small increases in pupil diameter. These characteristics are a very powerful indication that the primary cause of negative dysphotopsia is likely to be the primary image going dark at very large visual angles. The visibility of a shadow is also affected by other light that is scattered from ocular tissue and other features of the IOL (such as the lens edge, IOL regions outside the optics, and the haptics).

With "positive dysphotopsia", light that bypasses an IOL is not really described in the clinical literature as a potential source of unwanted bright light phenomena at night. This light is not focused by the IOL, and although it probably tends to blur into the general visual scene at night, it has relative motion, and a different shape, compared to the primary image of a light source. There are often reports of visual phenomena at night, and it is possible that the double image characteristic described here may be involved with those types of report. The PSF images here illustrate that there can be a double image even for visual angles as low as 50^0. The primary cause of bothersome positive dysphotopsia is actually total internal reflection at the edge of an IOL, which is not the mechanism evaluated here.

All these types of visual phenomena may be thought of as artifacts of the IOLs, or of the surgery, but they are also fundamental characteristics of the imaging system of the pseudophakic eye. These details are not usually described in this manner, which is probably because of the tolerance of the visual system to visual phenomena anyway, and perhaps also because patients with IOLs have previously experienced vision with cataracts, and may have become tolerant of a higher level of visual disturbance. Informing patients pre-operatively about the possibility of visual phenomena may allay concerns later if anything is noticed. This could include comments that there may sometimes be dark shadow regions with an IOL in the far periphery, and that most people are not bothered by these at all, but even if noticed initially, after a short amount of time they are usually not noticed. Even if they persist though, they have a known cause, and they are not a sign of any additional disease.

It should also be possible to generate images that depict a shadow using a physical model eye, though there do not yet appear to be publications that include these. Capturing the image that is formed on the highly curved retinal surface using an electronic sensor is particularly complicated, because most image sensors are flat, and they are also not normally used in contact with fluid. One method for capturing the retinal image is to use a fiber-taper, where a solid matrix of optical fibers that can relay an optical image is constructed so that the fibers become smaller and closer together at one end. The tapered region is ground at the smaller diameter end to have a radius of curvature that is similar to the retina, and this is used in fluid at the retinal location, with a relay lens and camera used to capture the plane image at the large end of the taper. This type of system has been described for use with lower visual angles [20] , [18] (with more detail in cited material A), and the same fiber tapers could probably be used for large visual angles if they were rotated, rather than being centered on-axis. The fiber taper has some additional complications, since the acceptance angle and transmittance can vary with input angle at the retinal end, and the relay lens at the output end also needs to capture all the light. A simplified alternative was also recently described, where a planar camera detector was immersed in fluid at the retinal location [21]. The detector was rotated to different angular locations, though not to the very large angles considered here. It may be possible to create a composite image using multiple images from different retinal locations, particularly because image resolution is very poor in the far periphery. These methods may also need to pay attention to the details of the peripheral cornea. The imaging characteristics of the peripheral

cornea may not have been specifically verified, and modeling the cornea using PMMA, which is a material that is often used, may have more complications than when the same material is used for more foveal imaging.

The intensity of the images generated here was adjusted radially using a cosine factor. Earlier papers that evaluated retinal luminance of the phakic eye noted that the increasingly elliptical shape of the pupil aperture with increasing visual angle is offset to some extent by the shorter distance to the retina, so that the retinal intensity may remain relatively constant [22,23]. Comments about the effect of the iris thickness were also included in another paper [24], though details were not given. None of the earlier papers deal with the pseudophakic eye, or with the perceived image intensity, and the adjustment was used here in order to generate comparative images. The overall effects of aberrations and defocus were not specifically evaluated.

The various publications about the potential causes of negative dysphotopsia are generally not in conflict with the discussion here, and the earliest references did not specifically consider the darkening of the primary image in the periphery as a potential cause. The calculations here show that the main image can go totally dark before the limit of the retina is reached. Other publications discuss much more modest intensity adjustments, due to the residual lens capsule on the anterior surface of an IOL, or to effects from lens edges. One example uses optical modeling with the non-sequential capability of the Zemax software to evaluate this [13], with additional discussions in response to a letter [25].

A more recent paper also utilizes the non-sequential Zemax software [14]. This is linked to the use of perimetry to measure the visual effect of negative dysphotopsia, and to the use of a secondary IOL in the sulcus to mitigate its effect. A difference is found with perimetry between patients who were bothered by negative dysphotopsia, and other patients who weren't, though they were not matched controls [26,27]. However, one limitation of standard perimetry is that the subject identifies only that something was seen, and not where it was seen, which may limit the ability to evaluate characteristics relating to a double image in the far periphery. Also, the pupil diameter when negative dysphotopsia is perceived is thought to be very small, which is not normally the case with perimetry. These papers are very useful, but the visual angles at which differences are seen with perimetry are smaller than the calculations in this paper, which may be because it is a related effect, but not actually the dark shadow location. The actual angles at which the patients perceive dark shadows are not given.

Another aspect of this discussion is the use of a piggyback IOL to reduce the visual effects of negative dysphotopsia [14,16,26]. This is considered to be effective in reducing the symptoms, and recent calculations for 3 specific patients where a silicone secondary IOL is used indicates that one effect is to move the iris forwards, which permits light from lower visual angles to bypass the original IOL, which in turn creates additional illumination of the peripheral retina [16]. In the paper mentioned above where an acrylic IOL is used, however [14], the beneficial effect is less clear in the theoretical calculations. The retinal irradiance plots there seem to show that the main image intensity declines at about 80^0- 90^0 of visual angle, which is in broad agreement with the calculations here (though it is not known if a difference of 5^0 between the optical and visual axis is being used). The other evaluations compared the ratios of intensities for the 60-70^0 to 20-30^0 regions however, indicating that the addition of a secondary "piggyback" lens made an intensity difference in that region. The calculation was compared to whether negative dysphotopsia was resolved, however, rather than to objective measurements for the same pupil diameter using the perimeter.

Evaluating this topic from a different perspective, it has not been shown that it is possible for light entering the pseudophakic eye at vary large visual angles to pass through an IOL to form an image. The topic does not seem to have been evaluated before the recent discussions relating to dark shadows. Raytrace evaluations indicate that at large input angles the light simply doesn't go through the IOL at all. If there is no image, then there is darkness (except that light can also miss the IOL in this situation, and illuminate the peripheral region). Even without total darkness, a rapid variation in peripheral image intensity may also be perceived as a shadow, though the sensitivity of the eye to this is not known.

The main images in Fig. 7 are for an average eye, but in practice there would be a lot of variation from patient to patient. Keeping the same basic eye, the effects of changing the iris thickness, changing the centration of the iris and the IOL, and tilting the IOL, were illustrated for certain parameter values in Fig. 8 and Fig. 9. These indicate that the location and magnitude of the shadow can vary with these parameters. The effect of typical iris thickness characteristics were included, but this itself is based on new information, and this parameter is not normally included in optical modeling. The iris thickness appears to have an effect on the far peripheral image of the pseudophakic eye, but it is not known yet which of the parameters contribute most to bothersome dark shadows. A related anatomical parameter is the clarity of the peripheral cornea, since corneal opacity may also occlude peripheral rays. Many parameters have never been measured for patients with negative dysphotopsia, and some do not appear to have ever been measured at all. The calculations here show that peripheral dark shadows are expected with IOLs, and systematic data collection relating to the shadows should show which parameters lead to the strongest visual phenomena.

Overall, the modeling here is in good agreement with clinical data. The main shadow is due to the IOL being too small to pass light at large angles, and the primary image goes dark at about 80^0 -85^0 of visual angle. This corresponds to the clearest reports of the phenomenon. The effect is strongest with a small pupil, and it decreases in effect as the pupil opens up, allowing additional light to bypass the IOL and illuminate the retina directly. Presenting normalized images on a polar plot that represents retinal location in object space, with intensity adjustments for a cosine falloff of intensity with angle, seems to be beneficial in illustrating the effect. This involves a visual region of the eye where there appears to be limited scientific knowledge, but objective measurements of shadow characteristics, and comparisons to simulated images, should ultimately confirm the cause.

.

Acknowledgments.
Grateful thanks to Maria Muzyka-Woźniak MD, Wroclaw, Poland, for the OCT images in Figure 1.

Portions of this work were presented at the 9th Visual and Physiological Optics meeting, Athens, Greece, 29-31 August 2018, p122.

References

1. P. J. Buckhurst, S. A. Naroo, S. Shah, T. Drew, and J. S. Wolffsohn, "Assessment of dysphotopsia in pseudophakic subjects with multifocal intraocular lenses," BMJ Open Ophthalmol. **1**, e000064 (2017).
2. M. J. Simpson, "Mini-review: Far peripheral vision. Vision Research," Vision Res. **140C**, 96–105 (2017).
3. R. H. Osher, "Negative dysphotopsia: long-term study and possible explanation for transient symptoms.," J. Cataract Refract. Surg. **34**, 1699–707 (2008).
4. J. T. Holladay, H. Zhao, and C. R. Reisin, "Negative dysphotopsia: the enigmatic penumbra.," J. Cataract Refract. Surg. **38**, 1251–65 (2012).
5. B. A. Henderson and I. I. Geneva, "Negative dysphotopsia: A perfect storm," J. Cataract Refract. Surg. **41**, 2291–2312 (2015).
6. M. J. Simpson and M. Muzyka-Woźniak, "Iris characteristics affecting far peripheral vision and negative dysphotopsia," J. Cataract Refract. Surg. **44**, 459–465 (2018).
7. C. E. Jones, D. A. Atchison, R. Meder, and J. M. Pope, "Refractive index distribution and optical properties of the isolated human lens measured using magnetic resonance imaging (MRI)," Vision Res. **45**, 2352–2366 (2005).
8. M. J. Simpson, "Double image in far peripheral vision of pseudophakic eye as source of negative dysphotopsia," J Opt Soc Am A **31**, 2642–2649 (2014).
9. M. J. Simpson, "Vignetting and negative dysphotopsia with intraocular lenses in " far peripheral vision ,"" J. Opt. Soc. Am. A **32**, 1672–1677 (2015).
10. J. T. Holladay and M. J. Simpson, "Negative dysphotopsia: Causes and rationale for prevention and treatment.," J Cataract Refract Surg **43**, 263–275 (2017).
11. S. Masket and N. Fram, "Etiology of negative dysphotopsia.," J. Cataract Refract. Surg. **39**, 485–6 (2013).
12. S. Masket, N. R. Fram, A. Cho, I. Park, and D. Pham, "Surgical management of negative dysphotopsia," J. Cataract Refract. Surg. **44**, 6–16 (2018).
13. X. Hong, Y. Liu, M. Karakelle, S. Masket, and N. R. Fram, "Ray-tracing optical modeling of negative dysphotopsia," J Biomed Opt. **16**, 125001-1–7 (2011).
14. N. Y. Makhotkina, V. Dugrain, D. Purchase, T. T. J. M. Berendschot, and R. M. M. A. Nuijts, "Effect of supplementary implantation of a sulcus-fixated intraocular lens in patients with negative dysphotopsia," J. Cataract Refract. Surg. **44**, 209–218 (2018).
15. M. Suheimat, H. Zhu, A. Lambert, and D. A. Atchison, "Relationship between retinal distance and object field angles for finite schematic eyes," 1–7 (2016).
16. J. C. Erie, M. J. Simpson, and M. H. Bandhauer, "Effect of a sulcus-fixated piggyback IOL on negative dysphotopsia: A ray-trace analysis," J Cataract Refract Surg Dec 18. pii: S0886-3350(18)30952-0. doi: 10.1 (2018).
17. J. C. Erie, M. J. Simpson, and M. H. Bandhauer, "A modified intraocular lens design to reduce negative dysphotopsia," J Cataract Refract Surg Submitted (2018).
18. K. K. Das, L. Werner, S. Collins, and X. Hong, "In vitro and schematic model eye assessment of glare or positive dysphotopsia-type photic phenomena: Comparison of a new material IOL to other monofocal IOLs," J. Cataract Refract. Surg. S0886-3350(18)30839–3, 1–9 (2018).
19. A. Mathur, J. Gehrmann, and D. Atchison, "Pupil shape as viewed along the horizontal visual field," J. Vis. **13**, 1–8 (2013).
20. A. Arianpour, E. J. Tremblay, I. Stamenov, J. E. Ford, D. J. Schanzlin, and Y. Lo, "An Optomechanical Model Eye for ophthalmological refractive studies," J Refr Surg **29**, 126–132 (2013).
21. S. Tsoukalas, P. Zafirakis, P. Artal, and H. Ginis, "A physical model of the pseudophakic eye for the study of wide-angle intraocular lens optics," in *Proceedings of 9th European Meeting on Visual and Physiological Optics, 29-31 August, Athens, Greece* (2018), pp. 229–232.
22. A. C. Kooijman, "Light distribution on the retina of a wide-angle theoretical eye," J Opt Soc Am A **73**, 1544–1550 (1983).
23. K. P. Pflibsen, O. Pomerantzeff, and R. N. Ross, "Retinal illuminance using a wide-angle model of the eye," J Opt Soc Am A **5**, 146–150 (1988).
24. A. C. Kooijman, F. K. Witmer, and K. Oogheelkunde, "Ganzfeld light distribution on the retina of human and rabbit eyes : calculations and in vitro measurements Ganzfield light distribution on the retina of human," J Opt Soc Am A **3**, 2116–2120 (1986).
25. X. Hong, Y. Liu, M. Karakelle, S. Masket, N. R. Fram, and J. T. Holladay, "Negative dysphotopsia: DIfferences in the studies of an enigmatic optic phenomenon (letters)," J Cataract Refract Surg **39**, 484–486.e3 (2013).
26. N. Y. Makhotkina, T. T. J. M. Berendschot, H. J. M. Beckers, and R. M. M. A. Nuijts, "Treatment of negative dysphotopsia with supplementary implantation of a sulcus-fixated intraocular lens," Graefe's Arch. Clin. Exp. Ophthalmol. **253**, 973–977 (2015).
27. N. Y. Makhotkina, T. T. J. M. Berendschot, and R. M. M. A. Nuijts, "Objective evaluation of negative dysphotopsia with Goldmann kinetic perimetry," J. Cataract Refract. Surg. **42**, 1626–1633 (2016).